

Biophysical Journal, Volume 113

Supplemental Information

Real-Time Imaging of a Single Gene Reveals Transcription-Initiated Local Confinement

Thomas Germier, Silvia Kocanova, Nike Walther, Aurélien Bancaud, Haitham Ahmed Shaban, Hafida Sellou, Antonio Zaccaria Politi, Jan Ellenberg, Franck Gallardo, and Kerstin Bystricky

Supporting Material

Real-time imaging of a single gene reveals transcription-initiated local confinement

Running title: Real-time single gene tracking

Thomas Germier^{1, §}, Silvia Kocanova^{1, §}, Nike Walther², Aurélien Bancaud³, Haitham Ahmed Shaban^{1, 4}, Hafida Sellou¹, Antonio Zaccaria Politi², Jan Ellenberg², Franck Gallardo^{1, 5, 6} and Kerstin Bystricky^{1, 5, #}

1 : Laboratoire de Biologie Moléculaire Eucaryote (LBME); Centre de Biologie Intégrative (CBI); Université de Toulouse; CNRS; UPS; 31062 Toulouse, France

2: Cell Biology and Biophysics Unit, European Molecular Biology Laboratory (EMBL), Meyerhofstr. 1, 69117 Heidelberg, Germany

3: Laboratoire de Automatismes et Architecture des Systèmes(LAAS); CNRS; UPS; 31000 Toulouse, France

4 : Spectroscopy Department, Physics Division, National Research Centre, El-Bohouth Str., 12622, Dokki, Giza, Egypt

5: Institut des Technologies Avancées du Vivant (ITAV); Université de Toulouse; CNRS; UPS; INSA; 31000 Toulouse, France

6: NeoVirTech S.A.; 31000 Toulouse, France

§: authors contributed equally

#: corresponding author: kerstin.bystricky@ibcg.biotoul.fr

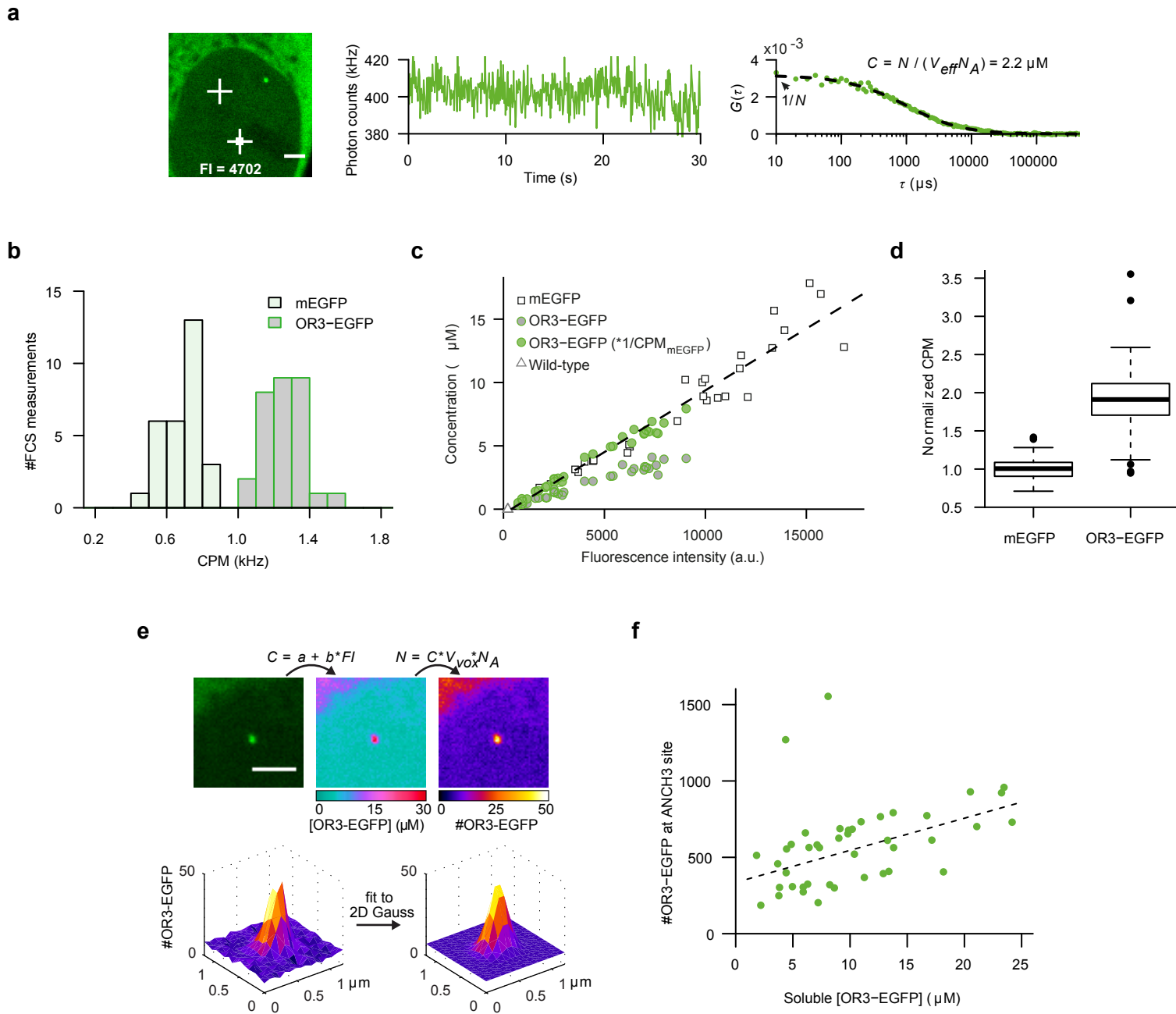


Fig. S1 (related to Fig.1): Biophysical characterization of ANCHOR3 fluorescent foci (a) Cells were imaged with the same laser and detector settings as for FRAP. Subsequently, photon counts were recorded at two non-ANCHOR nuclear positions. The mean fluorescence intensity of a 5x5 px region at the FCS point (FI, indicated) was extracted from the image (left panel). From the photon counts at the FCS point (central panel) the autocorrelation function was computed and fitted to a single component diffusion model according to Eq. S2 (see supplementary materials and methods (supMM)) in order to obtain the number of molecules N in the effective volume V_{eff} and the concentration C (right panel, N_A : Avogadro's number). (b) Photon counts per molecule (CPM) for mEGFP and OR3-EGFP expressing cells from one experiment. For OR3-EGFP (1.24 ± 0.11 kHz, $n=30$ FCS measurements) counts almost doubled compared to mEGFP (0.68 ± 0.1 kHz, $n=29$ FCS measurements), reflecting OR3-EGFP dimerization. (c) The concentrations obtained from FCS as function of the fluorescence intensity at the FCS location are plotted for OR3-EGFP, mEGFP and wild-type cells from one experiment. The CPM scaled concentrations for OR3-EGFP (green filled circles) align with the concentrations for mEGFP (grey rectangles). The calibration curve (Eq. S3) is shown as dashed line ($a=-0.368 \mu\text{M}$, $b=9.75e-4 \mu\text{M}$). (d) CPMs for mEGFP and CPMs for OR3-EGFP normalized to the mean CPM values of mEGFP are plotted ($n > 45$ cells per condition, 4 experiments with $n \geq 9$ cells per experiment). The boxplot shows median, lower and upper quartile, and $1.5 \cdot \text{IQR}$ (inter quartile range, whiskers). (e) The fluorescence intensity of the first pre-bleach frame of the FRAP time-course (left panel) was converted to a concentration using Eq. S3 (central panel). The concentration was converted to protein number by multiplying the concentration with the voxel volume $V_{vox} = \Delta x \Delta y \Delta z$ and the Avogadro's constant N_A (right panel). The protein number profile at the ANCHOR3 spot was fitted to a 2 dimensional Gaussian function (Eq. S4) and the total protein number was extracted. (f) The OR3-EGFP protein number at the ANCHOR site is plotted as a function of the soluble OR3-EGFP concentration in the nucleus. Scale bars: $2 \mu\text{m}$.

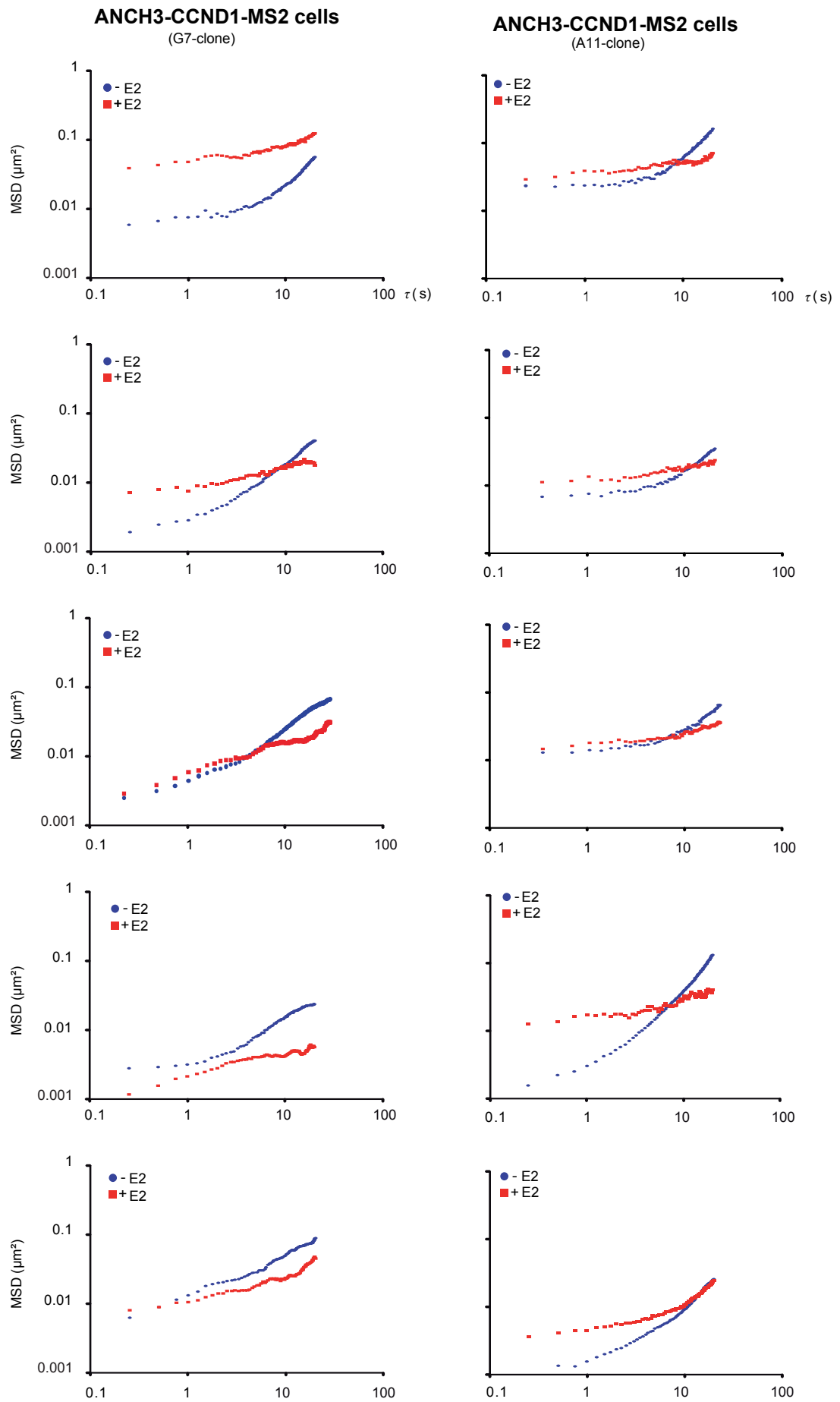
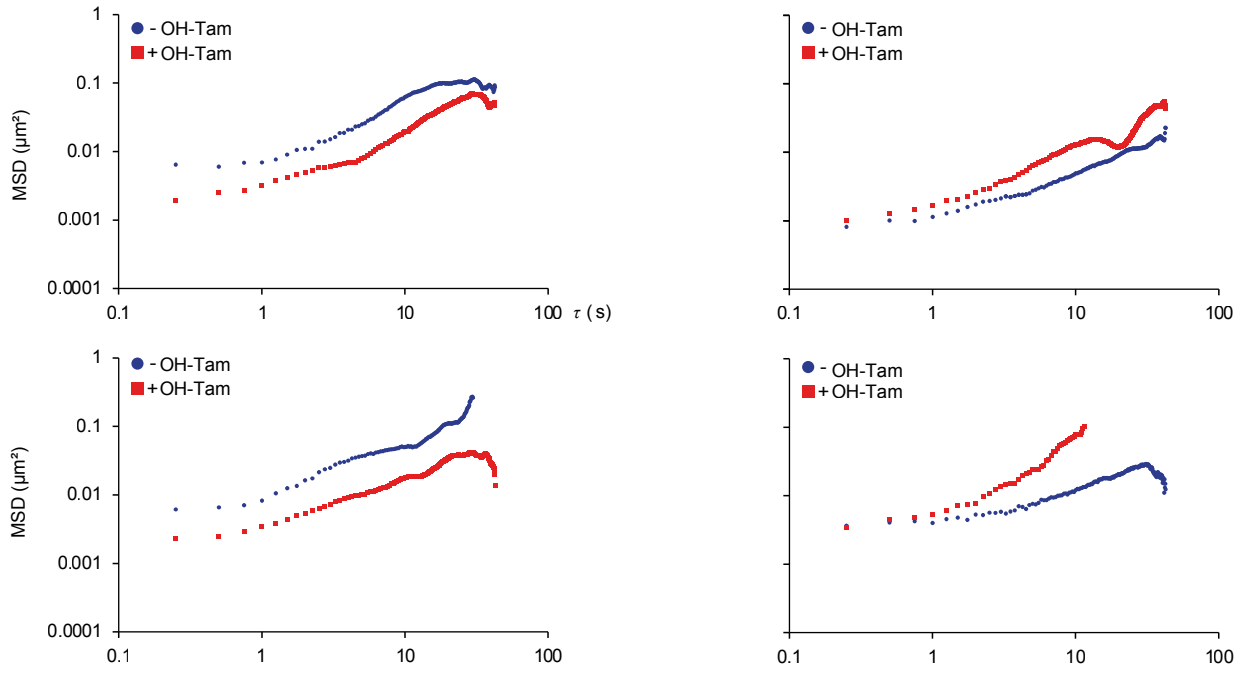


Fig.S2 (related to Fig.2): Motion of the ANCHOR3-tagged CCND1 locus is confined during estradiol activated transcription in single cells. Single cell MSD curves of OR3-Santaka loci in ANCH3-CCND1-MS2 cells at two different chromosomal insertion sites (clones G7 and A11; distinct stable FRT insertions in MCF-7 cells) before and 45 min after E2 addition. The movies to track CCND1 loci were acquired with an exposure time of 200 ms at 250 ms intervals.

a**ANCH3-CCND1-MS2 cells**

(D11-clone)

**ANCH3-CCND1-MS2 cells**

(G7-clone)

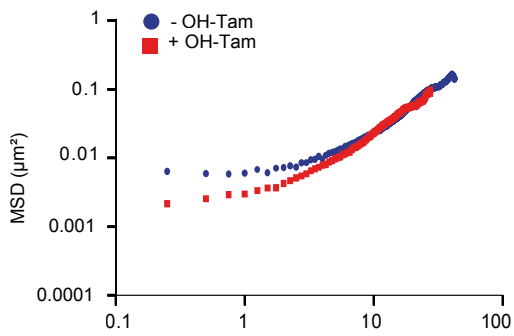
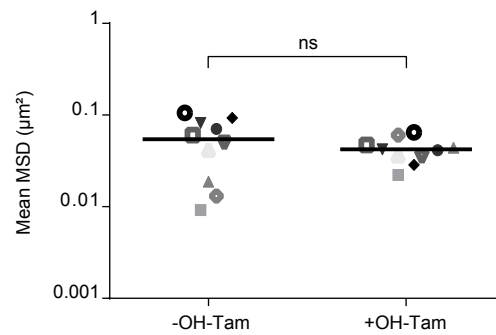
**b**

Fig. S3 (related to Fig.3): OH-Tamoxifen (OH-Tam) does not alter CCND1 locus dynamics.

The movies of CCND1 loci in ANCH3-CCND1-MS2 cells were acquired with an exposure time of 200 ms at 250 ms intervals over 50 s before and 45 min after addition of 1 μ M OH-Tam. (a) Single cell MSD curves of OR3 loci at two different chromosomal insertion sites (clones D11 and G7; stable FRT insertions in MCF-7 cells) are shown. (b) Average squared displacement between 2 s and 40 s (mean MSD) of tracking of the OR3-Santaka spot in ANCH3-CCND1-MS2 cells (n=10) before and 45 min after OH-Tam addition.

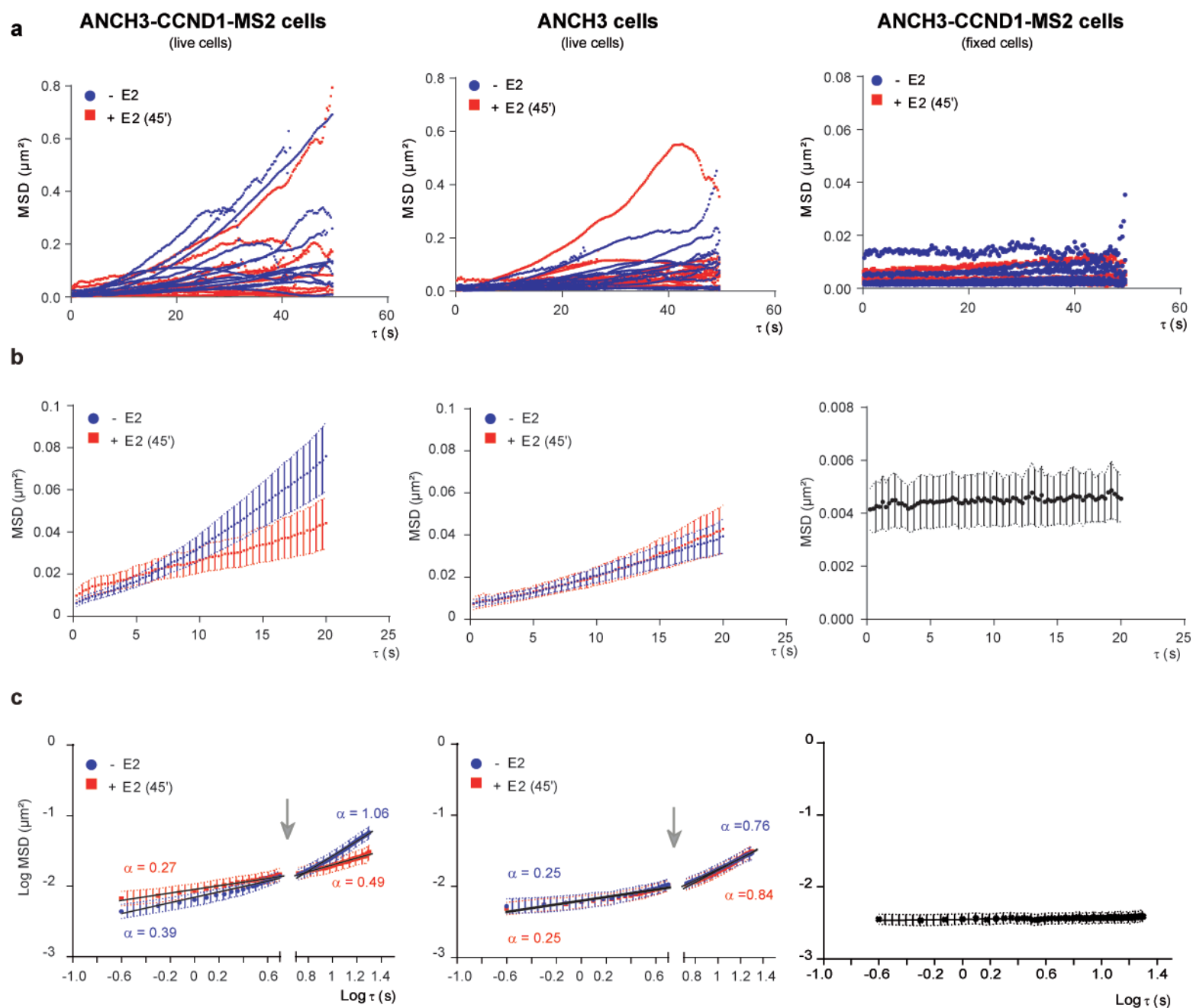


Fig.S4 : Linear fit of the two regimes of the averaged MSD
(a) All raw single cell MSD curves (left and middle panel, $n=14$ for ANCH3-CCND1-MS2 and ANCH3 cells; right panel, $n=6$ for ANCH3-CCND1-MS2 fixed cells (experimental error measurement)); (b) Averaged MSD cut at $\tau=20$ s before and after E2 addition presented in linear scale. (c) Transformation of averaged MSD in Log/Log scale allows a linear fitting on the two different regimes composing the curves. The arrow indicates the 5 s time point separating two diffusive regimes. The first fit is applied from $\tau=\text{Log}(0.250)$ to $\tau=\text{Log}(5)$ and the second fit is applied from $\tau=\text{Log}(5.250)$ to $\tau=\text{Log}(20)$ showing two different anomalous exponents α .